Notes

Solvothermal Construction of a Coordination Polymer around in Situ Generated Pyroglutamic Acid: Preparation, Crystal Structure, and Magnetic Behavior of $[Mn(C_5H_6NO_3)_2]_\infty$

Siegfried O. H. Gutschke, Daniel J. Price,† Annie K. Powell,‡ and Paul T. Wood*

School of Chemical Sciences, University of East Anglia, Norwich NR4 7TJ, U.K.

Received October 25, 1999

Hydrothermal and solvothermal[1] methods have been extensively employed to generate solid-state oxides,[2] e.g., zeolites, phosphates,[3] and chalcogenides.[4] Similar methods have also recently been employed to prepare infinite metal−ligand frameworks.[5−8] We have shown that carboxylates[7] and similar ligands[8] can be used to construct unusual crystal architectures under solvothermal conditions and wished to extend this to amino acids as compounds from the chiral pool are attractive starting materials for preparing chiral solids. We now report the results of a preliminary study in which we have focused on racemic starting materials.

Experimental Section

Synthesis. Manganese bis(pyroglutamate) **1** was prepared by placing a mixture of manganese(II) chloride tetrahydrate (250 mg, 1.99 mmol), D,L-glutamic acid (354 mg, 2.52 mmol), pyridine (666 mg, 8.42 mmol), and methanol (6 mL) in a 23 mL Teflon-lined autoclave and heating to 180 °C for 24 h. The reaction mixture was then allowed to cool to room temperature over a period of 4 h. The large colorless crystals were filtered, washed with methanol, and air-dried (yield 0.438 mg, 56%). Anal. Found: C, 38.60; H, 3.92; N, 8.99. $MnC_{10}H_{12}N_2O_6$ requires: C, 38.59; H, 3.88; N, 9.04. ν_{max} (KBr/cm^{-1}): 3262 s, 3022 w, 2981 w, 2970 w, 2939 w and 2880 w, 1707 s, 1651 s, 1605 s, 1566 s, 1443 s, 1416 s, 1362 m, 1313 s, 1290 m, 1260 s, 1206 w, 1150 w, 1101 w, 1041 w, 1022 w, 984 w, 925 w, 890 w, 842 w, 833 w, 788 w, 753 m, 717 s, 643 m, 559 w, 543 w, 507 m, and 474 m.

X-ray Crystallographic Analysis. A suitable crystal was mounted on a glass fiber and data collected on a Rigaku AFC7R diffractometer using graphite-monochromated Mo Kα radiation ($\lambda = 0.71073$ Å). Lorentz and polarization corrections and an empirical absorption correction were applied. The structure was solved by direct methods and refined using full-matrix least-squares on F^2. The hydrogen atom attached to nitrogen (H(10)) was found in a difference map and was refined isotropically; the other hydrogen atoms were placed in idealized positions and were allowed to ride on their parent atoms. All non-hydrogen atoms were refined anisotropically.

Magnetic Measurements. The field-cooled magnetic susceptibility of a powder sample was measured using a Quantum Design MPMS SQUID magnetometer. Data were collected in the range 5−300 K in an applied field of 1000 G. The sample susceptibility was corrected for diamagnetism, $\chi_{dia} = -128 \times 10^{-6}$ cm^3 mol^{-1} (calculated from Pascal's constants[9]).

Results and Discussion

The X-ray crystal structure (Table 1) shows that glutamic acid has undergone an intramolecular dehydration to form a lactam carboxylate. Dehydration reactions have previously been observed in superheated water.[10] Hence it is not too surprising that dehydration can also occur in superheated methanol. Particularly relevant to the current chemistry is the observation of esterification in superheated water. Condensation of glutamic acid also leads to the presence of pyroglutamate at the N terminus of some proteins.[11] It is notable that **1** is the only solid product of this reaction and no solid product incorporating the undehydrated ligand is observed. Heating for an additional day increases the yield to 65% but at the expense of the physical appearance of the product although IR spectroscopy and microanalysis show the product still to be of good quality. It is therefore possible that considerable quantities of soluble manganese glutamates may be present in solution even after prolonged heating. When pyroglutamic acid is used as the starting material in an otherwise identical reaction **1**, is again produced but in a lower yield and only after 2 days of heating. The reaction of manganese chloride with an authentic sample of pyroglutamic acid in the presence of base at room temperature does not lead to the formation of any solid products; therefore solvothermal conditions are necessary for the formation of the extended structure. Related reactions with a wide range of bases (e.g., LiOH, NaOH, $Ca(OH)_2$) under hydrothermal conditions do not lead to any solid products. In our hands this product may only be obtained for manganese and attempts to obtain analogues containing other divalent metal ions starting from both glutamic and pyroglutamic acid have been unsuccessful.

The ligand is coordinated to three different manganese atoms via all three oxygen atoms but not through nitrogen. This is in contrast to what we have observed for aromatic amine carboxylates[6,12] where the nitrogen is always coordinated. The complex forms well-separated infinite chains which run along the crystallographic *c* axis (see Figure 1). Bridges between adjacent manganese atoms are formed both by the carboxylate functions and via a longer pathway, through both ketone and carboxylate.

* Author to whom correspondence should be addressed. E-mail: p.wood@uea.ac.uk.

† Present address: Department of Chemistry, University of Southampton, Highfield, Southampton SO17 1BJ, U.K.

‡ Present address: Institut für Anorganische Chemie der Universität, D-76128 Karlsruhe, Germany.

(1) Rabenau, A. *Angew. Chem., Int. Ed. Engl.* **1985**, *24*, 1026.
(2) Barrer, R. M. *The Hydrothermal Chemistry of Zeolites*; Academic Press: London, 1982.
(3) Khan, M. I.; Meyer, L. M.; Haushalter, R. C.; Schweitzer, A. L.; Zubieta, J.; Dye, J. L. *Chem. Mater*. **1996**, *8*, 43.
(4) Wood, P. T.; Pennington W. T.; Kolis, J. W. *J. Am. Chem. Soc*. **1992**, *114*, 9233.
(5) Yaghi, O. M.; Li, H. *J. Am. Chem. Soc*. **1995**, *117*, 10401.
(6) Gutschke, S. O. H.; Slawin, A. M. Z.; Wood, P. T. *J. Chem. Soc., Chem. Commun*. **1995**, 2197.
(7) Gutschke, S. O. H.; Molinier, M.; Powell, A. K.; Winpenny, R. E. P.; Wood, P. T. *Chem. Commun*. **1996**, 823.
(8) Gutschke, S. O. H.; Molinier, M.; Powell, A. K.; Wood, P. T. *Angew. Chem., Int. Ed. Engl.* **1997**, *36*, 991.
(9) See, for example: Kahn, O. *Molecular Magnetism*; VCH: Weinheim, 1993.
(10) Katritzky, A. R.; Allin, S. M.; Siskin, M. *Acc. Chem. Res.* **1996**, *29*, 399.
(11) Stroble, S.; Gomis-Rüth, F.-X.; Maskos, K.; Frank, G.; Huber, R.; Glockshuber, R. *FEBS Lett*. **1997**, *409*, 109.
(12) Gutschke, S. O. H.; Gerrard, L. A.; Wood, P. T. Unpublished work.

10.1021/ic9912427 CCC: $19.00
Published on Web 07/14/2000

Table 1. Crystal Data for **1**

formula	$C_{10}H_{12}N_2O_6Mn$	space group	*C*2/*c*
a, Å	13.124(3)	*T*, °C	−40
b, Å	10.028(2)	λ, Å	0.71073
c, Å	8.237(1)	ρ_{calc}, g cm^{-3}	1.907
β, deg	90.77(2)	μ, mm^{-1}	1.246
V, Å^3	1083.9(3)	R1(F_o)[a]	0.0311
Z	4	wR2(F_o^2)[b]	0.0851
M	311.16		

[a] $R1 = \sum||F_o| - |F_c||/\sum|F_o|$. [b] $wR2 = [\sum w(F_o^2 - F_c^2)^2/\sum w(F_o^2)^2]^{1/2}$ where $w = 1/[\sigma^2(F_o^2) + 0.0264(F_o^2 + 3F_c^2)/3]$.

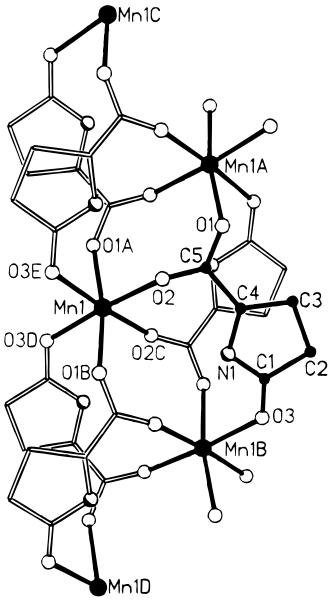

Figure 1. View of a small part of a manganese pyroglutamate chain showing the atom-numbering scheme. One ligand is highlighted using filled circles for carbon atoms and solid lines for bonds.

Table 2. Significant Bond Lengths (Å) and Angles (deg) for **1**

Mn(1)−O(1A)	2.176(2)	Mn(1)−O(2)	2.177(2)
Mn(1)−O(3D)	2.205(2)	C(5)−O(1)	1.249(3)
C(5)−O(2)	1.251(3)	C(1)−O(3)	1.249(3)
N(1)−C(1)	1.321(4)	N(1)−C(4)	1.469(3)

O(1A)−Mn(1)−O(1B)	170.2(1)	O(1A)−Mn(1)−O(2)	94.5(1)
O(1A)−Mn1−O(2C)	92.5(1)	O(1A)−Mn(1)−O(3E)	83.6(1)
O(1A)−Mn(1)−O(3D)	89.6(1)	O(2)−Mn(1)−O(2C)	89.0(1)
O(2)−Mn(1)−O(3E)	89.4(1)	O(2)−Mn(1)−O(3D)	175.7(1)
N(1)−C(1)−C(2)	108.8(2)	C(1)−C(2)−C(3)	103.7(2)
C(2)−C(3)−C(4)	104.9(2)	C(3)−C(4)−N(1)	102.3(2)
C(4)−N(1)−C(1)	114.7(2)		

The longer path also bridges between a manganese atom and its two next-nearest neighbors. The distance between adjacent manganese atoms is 5.086(2) Å. The environment around manganese is approximately octahedral with bond angles lying in the ranges 83.6(1)−94.5(1)° and 170.2(1)−175.5(1)°. Manganese−carboxylate distances are essentially equivalent (Mn1−O1, 2.176(2) Å; Mn1−O2, 2.177(2) Å) while the manganese−ketone bond is slightly longer (Mn1−O3, 2.205(2) Å) (Table 2). This difference is not mirrored in the C−O bond lengths, all three of which are identical within the error of the structure determination; hence the differences in Mn−O bond lengths may be attributed to packing forces rather than differing oxygen basicity. The delocalization of the nitrogen lone pair toward the ketone oxygen is illustrated by the large difference in bond lengths between nitrogen and the adjacent carbon atoms (N1−C4, 1.249(3) Å; N1−C1, 1.469(3) Å). The C1−N1−C4 bond angle is expanded to 114.7(3)°, between the values expected for tetrahedral and trigonal planar. The bond length and angle

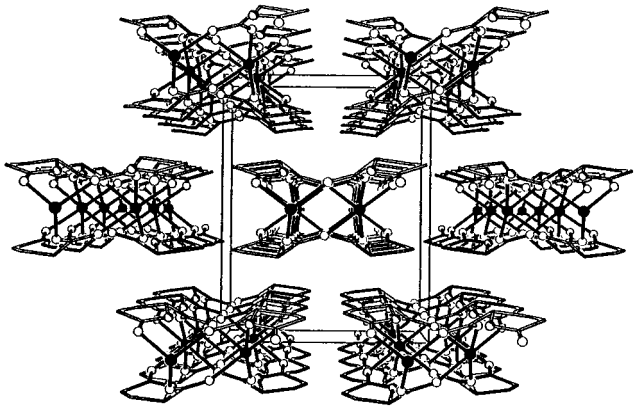

Figure 2. View down the crystallographic *c* axis showing the packing of chains.

data suggest approximately 50% delocalization of the lone pair. This is consistent with the lack of coordination via nitrogen.

The coordination around manganese can be viewed as consisting of two chelate rings and two monodentate ligands in the cis geometry with the rings formed by two pairs of carboxylates bridging to adjacent Mn atoms. As such the manganese atoms are chiral but each chain contains alternating Δ and Λ isomers. The conformation of the organic rings is such that a nonpolar hydrocarbon sheath is formed around the metal−oxygen core with the amine hydrogens also pointing into this area (see Figure 2). The nonpolar character of the polymer's outer surface may account for the absence of any lattice solvent molecules. We have noted in other cases[12] of solvothermal synthesis that materials with low-dimensional structures tend to yield crystals where this property is evident, i.e., 2-D structures often give flaky mica-like crystals and 1-D structures frequently lead to fibrous crystals. This is not the case with **1**, which gives robust and well-formed crystals despite the weak interactions between chains evident from its crystal structure.

High-spin manganese(II) in an octahedral crystal field has a $^6A_1$ ground term. This can be perturbed by both axial and rhombic distortions to produce a zero-field splitting, but this will be small; in general $|D| < 0.1$ cm^{-1}.[13] Consequently the spin anisotropy of this ion will be very low and we can expect isotropic or Heisenberg-like behavior. At room temperature the effective magnetic moment is consistent with a spin $^5/_2$ ion, and a plot of χ^{-1} vs T gives a straight line which can be fitted to Curie−Weiss law. The best fit was obtained using only the high-temperature data (in the range 40−300 K) and gave $C = 4.87(1)$ cm^3 mol^{-1} K^{-1} and $\theta = -7.7(1)$ K. The negative value of θ and the positive gradient of a graph of χT versus T is suggestive of an antiferromagnetic exchange interaction.

Structural considerations allow us to find likely models to account for the observed magnetism (see Figure 3). In general the shortest superexchange pathways mediate the strongest spin−spin interactions. In the structure of **1** we can see that the shortest pathways are provided by carboxylate bridges which link manganese ions into a one-dimensional zigzag chain. Not only are there no covalent pathways linking manganese ions in adjacent chains, but the shortest interchain Mn···Mn distance is 7.963(2) Å. Thus to a first approximation the interchain coupling should be negligible and the system will be well described by an exchange Hamiltonian. At the simplest level we can apply the result of Weiss's molecular field theory (MFT)[14] (eq 1) to the measured Weiss constant θ. This yields

(13) Mitra, S. *Prog. Inorg. Chem.* **1977**, *22*, 309.
(14) Carlin, R. L. *Magnetochemistry*; Springer-Verlag: Berlin, 1986.

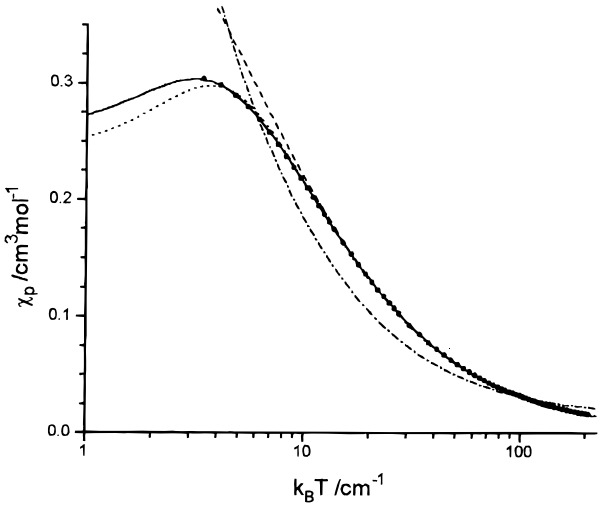

Figure 3. Graph of susceptibility versus thermal energy. Measured data are represented by large dots, behavior predicted by a simple Curie−Weiss model by long regular dashes, fits allowing for the effect of zero-field splitting by alternating dashes and dots, the model due to Weng by short dashes, and the model due to Fisher by a solid line.

$$\theta = 2S(S+1)zJ/3k_B \quad (1)$$

a coupling constant $J = -0.46(1)$ cm^{-1}. This is certainly a very crude approach as the MFT approximation is least satisfactory in the limit of low structural dimensionality, however it provides us with a magnitude for the exchange. There is no analytical solution for the Hamiltonian describing a 1-D chain of interacting spins; however there are numerical approximations which provide more sophisticated models. The most appropriate of these is the result of Fisher[15] (eq 2) obtained by treating the system as classical isotropic spins.

$$\chi_p = \frac{Ng^2\mu_B{}^2S(S+1)}{3k_BT}\left(\frac{1+u}{1-u}\right) \quad (2)$$

where

$$u = \coth[2JS(S+1)/k_BT] - k_BT[2JS(S+1)]^{-1}$$

Using this model we derive a value of $J = -0.376(1)$ cm^{-1}.

A second method has also been given by Weng.[16] He has numerically calculated the quantum behavior of a chain of antiferromagnetically interacting spins for different values of *S*. This behavior can be well described by a polynomial expansion[17] in $|J|/k_BT$. For $S = {}^5/_2$ the susceptibility is given by eq 3. A good fit to the experimental data is obtained yielding

$$\chi_p = \frac{Ng^2\mu_B{}^2}{k_BT}\left(\frac{2.9167 + 208.04(|J|/k_BT)^2}{1 + 15.543(|J|/k_BT) + 2707.2(|J|/k_BT)^3}\right) \quad (3)$$

a value of $J = -0.366(2)$ cm^{-1}. The zero field splitting of this ion is expected to be much smaller than the exchange coupling. However, it might also be a cause of the observed behavior; hence, we have attempted to fit the data with an axial splitting parameter, *D*. Given the low site symmetry of the manganese ion there almost certainly exists an additional rhombic splitting term, *E*; however, it was felt that if zero-field splittings were significant, then the axial model would provide at least a first approximation to the observed behavior. Least-squares refinement of this model did not converge well, and, in comparison with the other models, the fit is far from satisfactory.

The suitability of the chain models, in particular Fisher's classical equation, is evident. The reason for this lies in the nature of the manganese(II) ion; it has a large quantum spin number ($S = {}^5/_2$) and a small spin anisotropy due to negligible spin−orbit coupling. Both these facts tend to make the classical approximation a good model. The values for *J* we have found for the intrachain coupling of **1** are in good agreement and also consistent with the values found in other similarly bridged structures[18] and of the same order of magnitude as in other one-dimensional Mn(II) systems.[19]

Acknowledgment. We thank EPSRC for funding and UEA for a studentship (S.O.H.G.).

Supporting Information Available: Magnetic data including equations used and listings of measured and derived quantities. An X-ray crystallographic file, in CIF format, plus a thermal ellipsoid plot of the structure. This material is available free of charge via the Internet at http://pubs.acs.org.

IC9912427

(15) Fisher, M. E. *Am. J. Phys.* **1964**, *32*, 343.
(16) Weng, C. Y. Thesis, Carnegie Mellon University, Pittsburgh, PA, 1969.
(17) Hiller, W.; Strähle, J.; Datz, A.; Hamacik, A.; Hatfield, W.; ter Haar, L. E.; Gütlich, P. *J. Am. Chem. Soc*. **1984**, *106*, 329.
(18) (a) Cano, J.; Munno, G. D.; Sanz, J. L.; Ruiz, R.; Faus, J.; Lloret, F.; Julve, M.; Caneschi, A. *J. Chem. Soc., Dalton Trans.* **1997**, 1915. (b) Hong C. S.; Do, Y. *Inorg. Chem.* **1997**, *36*, 5684.
(19) See, for example: O'Connor,C. J. *Prog. Inorg. Chem*. **1982**, *29*, 203 and the references therein.